Warr, PA., Morris, KA., Watkins, GT., Horseman, TR., Takasuka, K., Ueda, Y., Kobayashi, Y., & Miya, S. (2009). A 60% PAE WCDMA handset transmitter amplifier. *IEEE Transactions on Microwave Theory and Techniques*, *57*(10, part 1), 2368 - 2377. https://doi.org/10.1109/TMTT.2009.2029021

A 60% PAE WCDMA Handset Transmitter Amplifier

Paul A. Warr, Kevin A. Morris, Gavin T. Watkins, Tony R. Horseman, Kaoru Takasuka, Yukihiro Ueda, Yasushi Kobayashi, and Shinji Miya

***Abstract*—This paper reports the design of a class-E envelope elimination and restoration (EER) based amplifier for a wideband code division multiple access handset application that attains 60% power-added efficiency at peak power output. Emphasis is placed on the envelope modulator that employs a novel split-frequency approach in order to attain an efficiency of 80% for this part of the system. In contrast to standard EER systems, the carrier is not amplitude limited, but rather predistorted to maintain both linearity and power efficiency. Performance in terms of efficiency, spectral output, and error vector magnitude is reported.**

***Index Terms*—Amplifier distortion, envelope elimination and restoration (EER), mobile communications.**

I. Introduction

THE WIDEBAND code division multiple access (WCDMA) waveform contains significant amplitude modulation: a peak-to-mean ratio of 3.5 dB means the signal is capable of generating large levels of distortion when amplified by an efficient, but nonlinear power amplifier (PA). Currently, power efficiency is compromised in order to meet the near-band spectral mask restrictions of this standard. The efficiency of a simple high-frequency amplifier increases as the output signal amplitude approaches the maximum current swing of the transistor. However, as this level is approached, the transistor will begin to distort the signal. With variable envelope signals, some of this distortion falls in-band, reducing the overall signal integrity, spreading the spectral energy, and in-channel, increasing error vector magnitude (EVM). Amplifier linearity and efficiency are, therefore, opposing goals, and it is necessary to address the linearity of the transmitter if efficiency is to be improved.

In a handset application, the complexity, efficiency, and implementation size of a linearization/efficiency enhancement scheme is of key concern. The majority of linearization schemes have been designed for base-station applications and do not suit the low power restrictions of a handset where feedback of the output signal is too costly. One solution to the handset PA efficiency/linearization requirement for the WCDMA (uplink) standard is to combine digital predistortion [1] with envelope elimination and restoration (EER) [2].

Manuscript received November 18, 2008; revised June 16, 2009. First published August 21, 2009; current version published October 14, 2009.

P. A. Warr, K. A. Morris, and T. R. Horseman are with the Centre for Communications Research, University of Bristol, Bristol BS8 1UB, U.K. (e-mail: ccr@bristol.ac.uk).

G. T. Watkins was with the Centre for Communications Research, University of Bristol, Bristol BS8 1UB, U.K. He is now with Toshiba Research Europe Limited, Bristol BS1 4ND, U.K.

K. Takasuka, Y. Ueda, Y. Kobayashi, and S. Miya are with the Asahi-Kasei EMD Corporation, Kanagawa 210-0863, Japan.

Digital Object Identifier 10.1109/TMTT.2009.2029021

TABLE I
PEAK POWER PAE OF PA MODULES FOR WCDMA HANDSETS

Manufacturer	PART NO.	Peak Power PAE (%)	Data source
Skyworks	SKY77152	37	Data Sheet
Skyworks	SKY77404	42	Preliminary only
Anadigics	CHP2299	40	Preliminary only
Maxim	MAX2291	37	Typical value only
RFMD	RF3137	40	Data Sheet
Agilent	ACPM-7833	38	Data Sheet
SiGe Semiconductor	SE5120	>40	Press release only
Fairchild	RMPA2259	40	Data Sheet
Fairchild	RMPA2265	40	Data Sheet
Toshiba	S-AL57	46	Press release only
TriQuint	TQM7M6001	40	Preliminary only
EiC corp	ECM060	43	Typical value only

In a standard EER amplifier system, the complex-modulated input signal is processed to form a phase-modulated signal at the RF carrier frequency, and an envelope signal is used to control the supply voltage of a gain device via a variable power supply (envelope modulator) with significant current delivery. The power supply modulation of the transistor reconstructs the waveform at the output. Several design issues prevail; e.g., the efficiency of the high current envelope delivery system is critical to the system efficiency, and the time alignment of the two signal paths is critical to the EVM performance [3].

The core PA device operating in a switching mode such as class E or F may theoretically operate with a power-added efficiency (PAE) approaching 100% and a WCDMA implementation is reported here that offers 24 dB of overall gain and peak PAE of 60% under WCDMA modulation at 26 dBm P_{OUT}. This represents a significant improvement of that available from commercial PA modules for the WCDMA handset application, as summarized in Table I. A relatively low gain is observed in all switching amplifier types due to the significant input voltage swing required to switch the device fully on and off. A driver amplifier (DA) is used here to overcome this low gain and its power consumption included in the efficiency calculation of the system.

II. High-Efficiency Polar Modulated PA Architecture

The voltage minima in the WCDMA RF waveform are of short time duration with steep gradients. In the EER amplification of this signal, the envelope path is required to have a high slew rate if these voltage minima are to be accurately reproduced. Incorrect reproduction will lead to a sub-optimum power supply voltage for a given input signal power.

Unlike many polar modulators, which drive the switching amplifier RF input with an amplitude-limited carrier [4], the solution reported here employs a partially envelope-modulated RF carrier at the amplifier's input. The class E amplifier is driven by

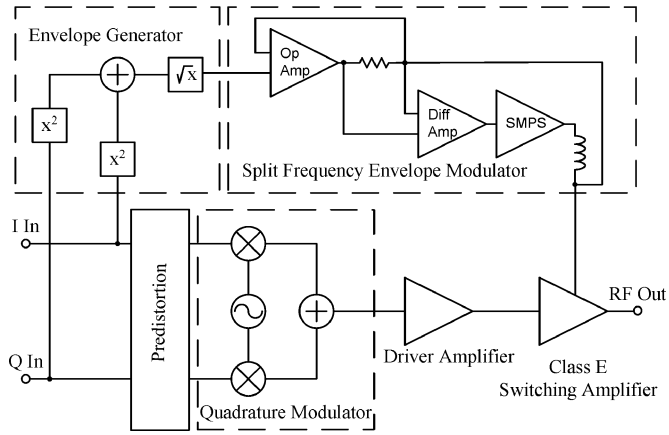

Fig. 1. EER amplifier. Amplitude predistortion is applied to the carrier at the input of the class E PA rather than a conventional amplitude-limited signal. The high-power envelope signal is applied to the bias of the PA via feedback-controlled linear op-amp and SMPS output signals.

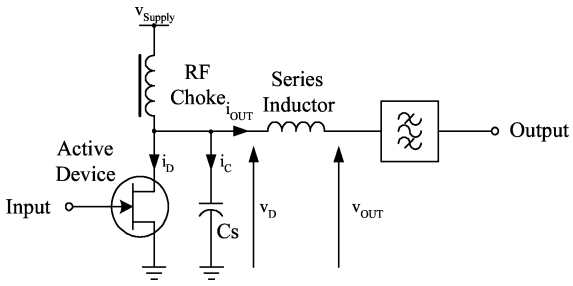

Fig. 2. Simplified class E amplifier architecture. The maximum switching frequency of the active device is high compared to the carrier frequency to ensure efficiency. A high filter Q is required for the standard design equations to be valid.

an input signal that tracks, in part, the supply voltage leading to an enhanced efficiency performance. Additionally, polar transmitters, which drive the switching amplifier with a constant envelope signal, suffer from the input signal leaking through the amplifier during the envelope nulls, causing signal phase and gain distortion. The solution presented here is immune to this form of distortion. There is an obvious complexity increase over the backoff solution to PA linearity; however, this facilitates the significant increase in efficiency observed with this solution.

The envelope signal is generated at baseband directly from the in-phase (I) and quadrature (Q) baseband signals. This allows an accurate magnitude signal to be calculated [5], as shown in Fig. 1.

III. Class E Switching Amplifier

Practical class E amplifiers have been shown to exhibit a PAE of 86% at 1.95 GHz [5]. This high level of efficiency can only be achieved by a switching amplifier architecture where there is very low power dissipation in the switching element.

The output bandpass filter of Fig. 2 is assumed to posses a high Q and have zero loss. A high-Q filter will ensure that all of the harmonics are reflected back into the amplifier instead of being dissipated in the load. The ideal design equations including a factor for the output filter Q of the class E amplifier are given in [6]. A reduced filter Q will lead to a detuning from the optimum component values.

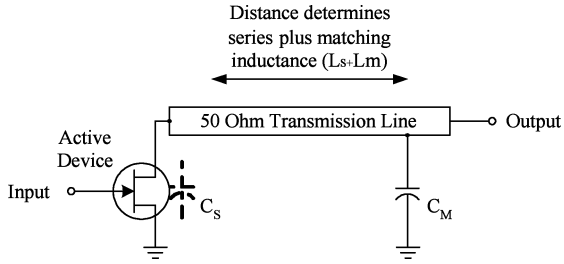

Fig. 3. Prototype class E amplifier output network. The transmission line approximates the required inductance that can not be realized without parasitic reactances at the carrier frequency.

At microwave frequencies, lumped inductors are lossy. Microwave frequency inductors should, therefore, be made from transmission line lengths, which offer very low loss, and hence, maintain a high Q.

The difficulties associated with developing a high-Q low-loss output bandpass filter may be circumvented by an alternative approach that employs a low-pass reactive network [7]. The class E amplifier will generally have low output impedance, and hence, require a matching network to match it to the nominal 50-Ω system impedance. A low-pass matching network with an identical Q to that of a series bandpass filter will provide similar harmonic zone impedances to the bandpass filter. If the series inductor of Fig. 2 and that of the matching network are replaced with a 50-Ω transmission line, then a simple transmission line architecture may be constructed.

A practical switching amplifier is realized using 50-Ω transmission lines for all series inductors since shunt capacitors may be moved along their length to vary the inductor's value. The impedance transforming action of these transmission line inductors complicates the design process since the transmission lines are not purely inductive. They also posses shunt capacitance proportional to their length. A simple L-section matching network based on a series transmission line inductance and a shunt capacitance may be used, as shown in Fig. 3.

During the tuning stage, with C_S as provided by the stray capacitance of the transistor, the matching capacitor (C_M) is varied while being moved along the 50-Ω transmission line. The impedance presented at the transistor's drain may be determined through measurement and simulation.

The ability to move the shunt capacitance along the length of the 50-Ω transmission line in this way allows the amplifier to be tuned for optimal performance. Preliminary tuning is carried out at the design and simulation station; but since the transistor model diverges from the idea small-signal characteristics under large-signal characteristics, a degree of manual tuning is required.

As the position along the transmission line and value of C_M are varied, the length of line used in the matching network will vary causing R_L to change, and hence, the Q. Since the optimum value of R_L is dependant on the output network's Q [as shown in (1)], a substitution can be made to remove R_L leaving only the Q, shown in (2) as follows:

$$R_L = 0.465\frac{V_D^2}{P_{\mathrm{OUT}}}\left[1 - \frac{0.452}{Q} - \frac{0.402}{Q^2}\right] \quad (1)$$

$$0 = Q^4 - 0.452Q^3 + 0.598Q^2 + 0.452Q - 0.402. \quad (2)$$

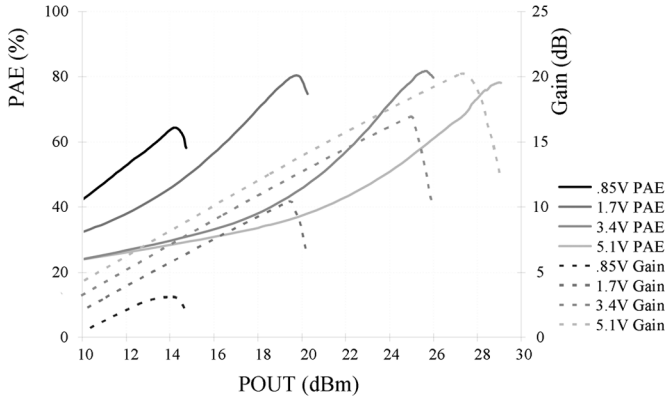

Fig. 4. 26-dBm class E amplifier characteristics at the mean voltage of 3.4 V, peak voltage of 5.1 V, 6-dB backoff (1.7 V), and 12-dB backoff (0.85 V).

For a designed $P_{\rm OUT}$ of 26 dBm, a 3.4-V $V_{\rm DS}$, and a 50-Ω system impedance, the optimum Q may be found graphically to be 2.04, equivalent to an R_L of 9.20 Ω. At 840 MHz, C_M is 7.2 pF assuming a 50-Ω transmission line is used for L_M. The electrical length of L_M will, therefore, be 23.4°. The exact values of C_S and L_S will be detuned by a low or moderate value Q

$$C_S = \frac{0.1836}{2\pi f_R R_L}\left[1 + \frac{0.914}{Q} - \frac{1.032}{Q^2}\right] \quad (3)$$

$$L_S = \frac{1.152 R_L}{2\pi f_R}\left[\frac{1.119Q - 0.187}{Q - 0.773}\right]. \quad (4)$$

Equations (1)–(4) are developed from [8].

C_S is calculated to be 4.5 pF and L_S is calcuated to be 3.89 nH. $Z_{\rm net}$, the required drain impedance produced by R_L and L_S, as $9.20 + 20.5j\Omega$. Since L_S is to be provided by a length of transmission line, it will not have a purely inductive component. This requires the recalculation of the matching network, which then becomes 21.6° for L_M and 8.0 pF for C_M. L_S is a 23.0° length of 50-Ω transmission line.

A. Practical Results Under Continuous Wave (CW) Excitation

Using the design equations, a 840-MHz 26-dBm amplifier was designed and tuned for maximum PAE. The amplifiers characteristics are shown in Fig. 4.

Fig. 4 shows data not just for a 3.4-V supply voltage, as supplied by the envelope modulator, but also for 5.1 V, the 3.5-dB envelope peak. 1.7 and 0.85 V, which are 6- and 12-dB backoff supply voltages, respectively. These results were achieved with 0-V gate bias to an ATF-501 transistor [9]; chosen because of an appropriate stray drain capacitance. Through simulation and experimentation, 0 V was found to be the optimum bias condition for class E operation. The amplifier exhibits a peak PAE of 81.6% at 25.7 dB $P_{\rm OUT}$ with 12.7-dB gain. The PAE decreases with reduced supply voltage, as expected due to the class E amplifier's nonlinear gain characteristic. The transistor will always need sufficient input signal power to switch it fully between saturation and isolation, regardless of the supply voltage.

The schematic of the 26-dBm 840-MHz transmission line amplifier is shown in Fig. 5. An output impedance of $9.20 + 20.5j\Omega$ is presented to the ATF-501P8 (LPCC package) transistor by the 4-pF capacitor (C_M) and 45° length of transmission line. According to the calculations above, C_M should be 8 pF. Practically, due to stray parasitic reactances, 4 pF proved optimum for C_M. The input matching network comprising the 5-pF capacitor and 56° transmission line proved optimum for the configuration used with 0-V bias.

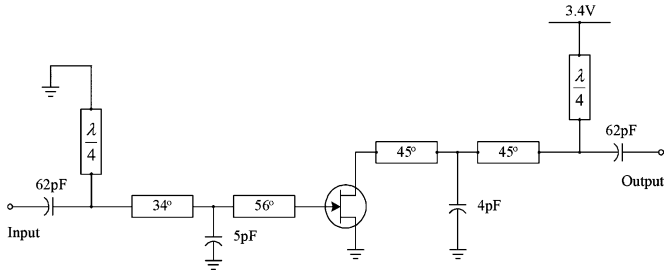

Fig. 5. 26-dBm class E amplifier schematic. The output semidistributed filter network is tuned for optimum PAE and gain at an output power of 26 dBm. Transmission lines are 50 Ω.

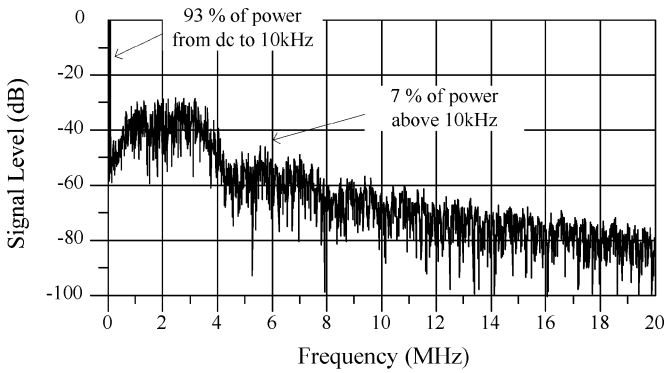

Fig. 6. Spectrum of WCDMA envelope magnitude. The majority of the signal energy is within the frequency range of SMPS architectures.

IV. Split Frequency Envelope Modulator

Switch mode power supplies (SMPSs) are well known for their efficient dc–dc conversion; however, the switching frequencies are under 1 MHz. The application of WCDMA envelope modulation by a SMPS means that it must be capable of switching at a rate well above the maximum significant spectral content of the envelope signal (circa 5 MHz, Fig. 6). Estimates from the literature suggest in the order of 20× the modulation bandwidth [10].

Modulating an SMPS with a WCDMA envelope signal is not feasible using current technology. The switching losses incurred due to the gate charge and the rise/fall times of the switching transistors lead to a low efficiency. A quasi-resonant topology could reduce these losses due to finite rise and fall times, but the drive losses associated with the gate charge can only be reduced by a half and complications arise due to the loss in the commutation diode.

The frequency distribution of the magnitude of the WCDMA envelope signal is shown in Fig. 6. The majority of the energy is located at dc with 93% of the power occurring below 10 kHz and 6.3% occurring above 500 kHz. This allows the SMPS to

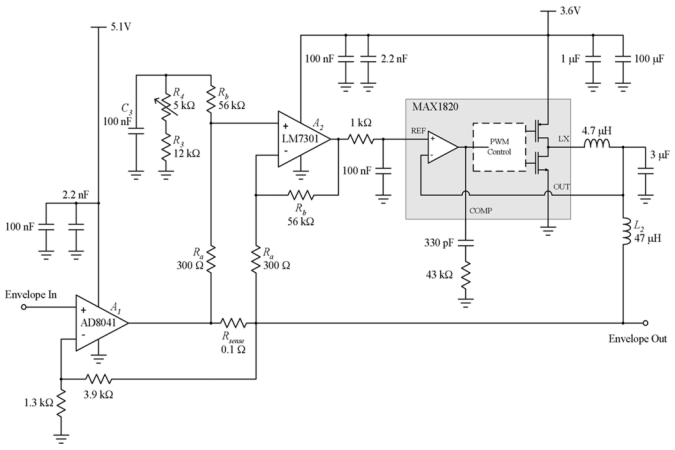

Fig. 7. Efficient envelope modulator circuit; a combination of an operational amplifier and low-frequency modulated SMPS. Feedback is used to ensure that the SMPS is supplying as much of the current at the output as possible, the remainder (higher frequency component) being supplied by the operational amplifier.

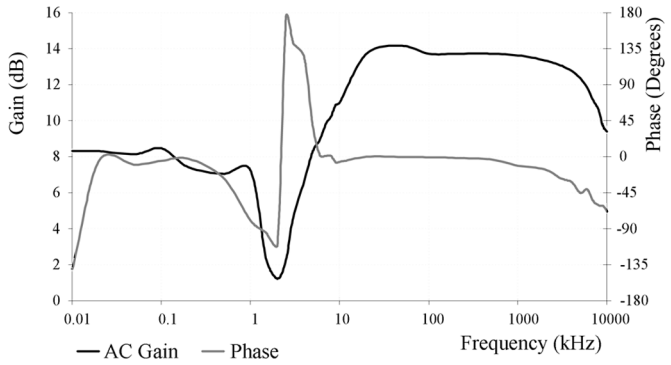

Fig. 8. Gain and phase response of the split-frequency modulator. The variation in gain with frequency is attributed to multiple feedback paths and is of little significance to the system.

efficiently amplify 93% of the energy. The remaining 7% of the envelope energy starts to roll off above 5 MHz. It is possible to take advantage of this by using a high-efficiency technique to generate the low-frequency or dc component and a low-power wide-bandwidth operational amplifier to apply only the high-frequency information.

The key issue is to find an efficient way to combine the two high-power envelope signals. In the solution proposed here, the two outputs are selectively combined in parallel. A suitable system as a starting point is introduced in [11] in which a generalized EER system is built around an X-band 10-GHz class E amplifier.

The architecture proposed in [11] is limited since the SMPS output does not lower the current output supplied by the linear regulator. A more efficient architecture is introduced here in Fig. 7. The feedback for the operational amplifier is at the output of the system so that the low-frequency current is supplied exclusively by the SMPS. This greatly lowers the current sink/source demands of the operational amplifier, and hence, a more efficient lower quiescent current device may be used.

The envelope modulator may be separated into two blocks: the SMPS with its current feedback loop and the operational amplifier with its voltage feedback loop. In addition to providing the current required so that the output voltage tracks the input at the higher frequency range, the closed-loop operational amplifier also compensates for any residual switching noise at the output of the SMPS because its feedback is taken from the output of the sub-circuit.

Signal combination is achieved by summing the currents from the SMPS and the operational amplifier circuit blocks. The SMPS supplies low-frequency current to the load through L_2. The operational amplifier A_1 acts as a current sink or source to apply the appropriate high-frequency ac waveform on to the SMPS's low-frequency output. At the operational amplifier operating frequency L_2 exhibits a high impedance, making the SMPS path approximate an ideal current source at high frequencies. Thus, current is summed at the output and is driven to the load impedance of the core amplifying device.

A. *Operational Amplifier*

Although the operational amplifier only has to supply 7% of the envelope power, this is the average power over a long period. The peak current sourced/sunk is significantly larger over short periods of time.

When the envelope signal experiences a null, the op-amp must sink the current supplied by the SMPS so as to pull the voltage at their combining node down to 0 V. Thus, it must be able to sink 161 mA. Similarly, at its peak output point, it must source 70 mA to raise the voltage to the 5.1-V peak. Sinking and sourcing such large currents is beyond the capabilities of most efficient op-amps. Even if an op-amp can supply the required current, there is often a significant voltage drop due to the high output impedance of the common emitter or common source output stages employed in rail-to-rail devices.

Other research into WCDMA polar modulator architectures [12] uses the OPA357 [13], which performs well, but does not have sufficient headroom for low-power battery operation. The AD8605 [14] is a very low power op-amp, with fairly good output current, but only a 10-MHz bandwidth. The AD8041 [15] is a good compromise between all performance characteristics, and has the excellent current sinking capability of 150 mA.

B. *SMPS*

The envelope modulator uses an MAX1820 SMPS integrated circuit (IC) [16], which is a 1-MHz Buck converter, to provide the large dc (and low frequency) component of the envelope signal around the mean output current. The MAX1820 is capable of supplying up to 600 mA for a 3.6-V input voltage and 3.4-V output voltage. Under these conditions, it is more efficient at supplying a large output current than a small one: the efficiency when supplying 22 mA is about 94%, while when supplying 161 mA (as required in this application), it is approximately 96%. This increase in efficiency is due to the quiescent current consumption of the SMPS.

A complicating factor with the SMPS IC is that it utilizes voltage feedback as part of the internal control loop. The output voltage is monitored to control the duty cycle. This internal path introduces a third feedback loop.

The gain and phase response of the complete split-frequency modulator is shown in Fig. 8. The dip in the gain response circa 2 kHz is due to the passive filters in the loop producing a 180°

phase shift between the two signal paths. Increasing the bandwidth and/or gain of the outer loop reduces this dip; however, the phase difference between the two loops leads to low-level oscillation on the output.

These problems may be avoided by using a single feedback loop around the SMPS, incorporating both the stabilization and output voltage control. This could be done by designing a discrete SMPS. However, with less than 0.06% of the total power occurring across the frequency range of concern, this poor low-frequency behavior has little effect on the measured efficiency and linearity results.

C. Current Feedback Loop

If the SMPS internal loop is removed, the *RC* low-pass network in the current feedback loop will set the bandwidth of the SMPS output.

The loop current gain is given by

$$G = G_{\mathrm{SMPS}} \frac{R_{\mathrm{sense}}}{R_L} \frac{R_b}{R_a} \tag{5}$$

where G_{SMPS} is the voltage gain of the SMPS IC (1.76 for the MAX1820), R_{sense} is the 0.1-Ω sense resistor, and R_L is the load resistance. R_a and R_b make up the current sense voltage divider.

By providing a floating bias point for the current sense amplifier, it is not necessary to have a gain greater than 1. C_3, R_3 and R_4 set up this floating bias point approximately 1.7 times lower than the average output voltage. This allows a lower loop gain to be used, which improves the noise immunity and stability of the system. The current sense amplifier gain was set to $56\ \mathrm{k}/300 = 45$ dB.

V. Polar Modulated PA Architecture Performance

A. Envelope Modulator Performance

The performance of the split-frequency modulator was measured when driven by a WCDMA envelope signal, which was varied to alter the output power level. At maximum output, the peak and mean output voltages are 5.1 and 3.4 V, respectively. With 5.1- and 3.6-V supply voltages efficiency is plotted in Fig. 9 when driving a 25-Ω resistor that models the class E amplifier's drain impedance.

The efficiency of the modulator increases as the output power increases due to the quiescent current consumption of the SMPS and operational amplifier, which become more significant as the overall power is reduced.

The operational amplifier is responsible for between 16% (at maximum output power) and 23% (at 15-dB backoff) of the total power consumption. By contrast, the ac component of the output power remains 6% of the total power regardless of output power. The operational amplifier will always be the weak point of the envelope modulator since even with ideal components, it can never be more than 67% efficient. Practically, the linear regulator is about 60% efficient.

In order to achieve optimum efficiency for a given operating power level, it is desirable to ensure that the net dc current flow into and out of the operational amplifier output is zero. By this measure, the device will not be supplying any dc current to the load or sinking any of the SMPS dc current. The SMPS current feedback loop ensures this by forcing any low-frequency current through the current sense resistor R_{sense} to zero. Modification of the network bias by adjustment of R_4 allows the current to be controlled.

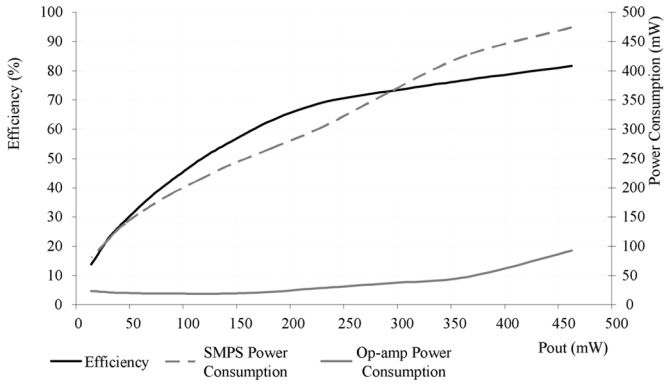

Fig. 9. Efficiency of the split-frequency modulator with a 25-Ω resistive load; a realistic approximation to the class E PA field-effect transistor (FET) drain. The input signal is the envelope extracted from a WCDMA signal.

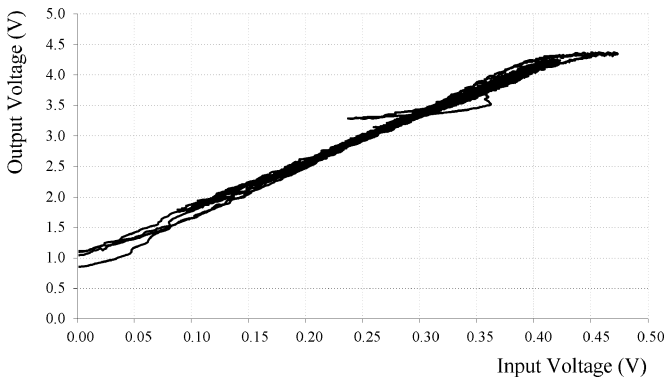

Fig. 10. Transfer function of the envelope modulator at maximum output power over a WCDMA packet. Variation of the gain profile in the frequency domain is indicated by the multiple trace paths across the output voltage range.

The voltage transfer function of the envelope modulator is shown in Fig. 10 across a 25-Ω resistor for maximum output power over a WCDMA packet. The spread of voltage mapping across a packet may be attributed to the frequency dependency of the gain response (Fig. 8).

The transfer function of the envelope modulator is fairly linear with a tight grouping of points in the middle third of the voltage range. At the upper input voltage range, the output voltage goes into compression as the linear regulator is unable to source sufficient current. There is a separation of the points in this region due to the linear regulator's feedback network being unable to correct for this compression. Similarly, at the lower end, the output voltage appears to have an offset of approximately 1 V due to the finite source resistance of the linear regulator.

The linear regulator has finite output impedance due to the common emitter output stage employed. This is especially prevalent when sinking current to produce the nulls. Due to the distortion introduced by the linear regulator, Fig. 10 appears to include an offset voltage.

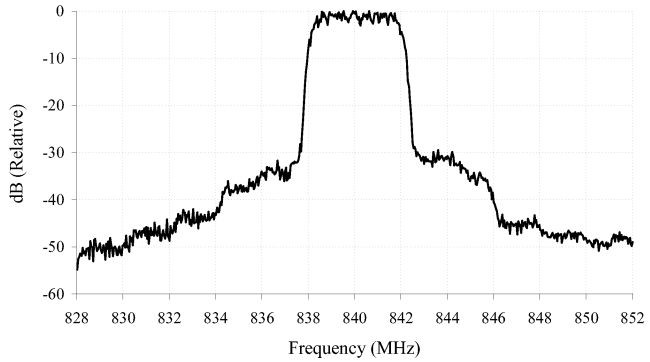

Fig. 11. Envelope modulator and class E output spectrum at 840 MHz. Gain is only 10.9 dB so a DA is required, which must also be efficient.

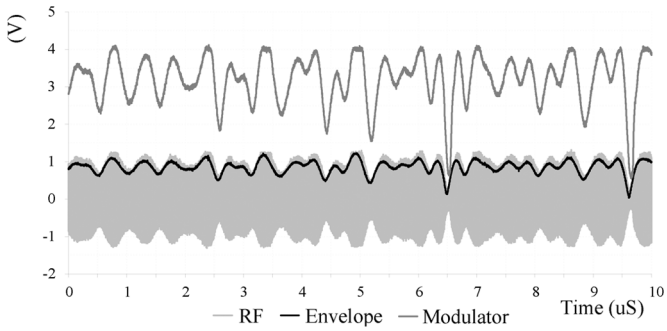

Fig. 12. Time-domain envelope waveforms. The accurate mapping of envelope to carrier is compromised by the use of a low quiescent current operational amplifier for the sake of system efficiency.

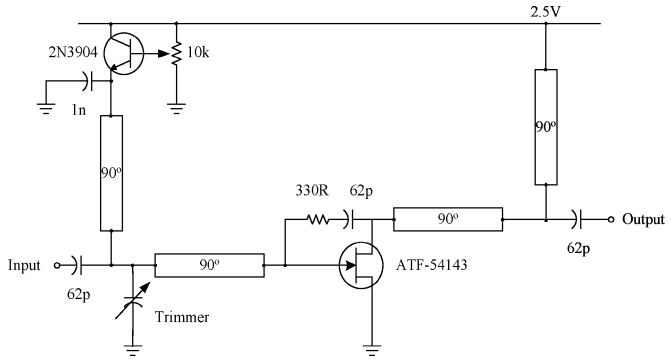

Fig. 13. Linear shunt feedback DA. The output impedance of the circuit is crucial for the attainment of efficiency in the subsequent PA. Transmission lines are 50 Ω.

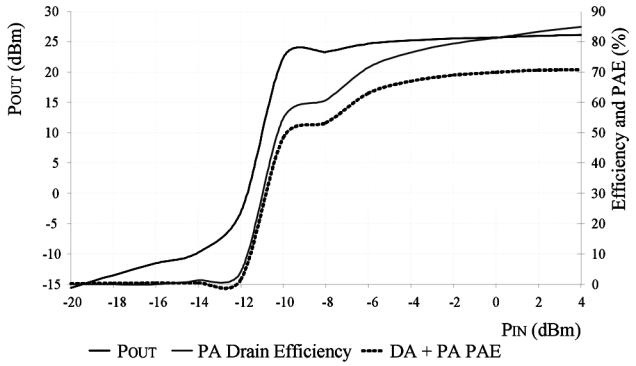

Fig. l4. Cascade amplifier CW transfer response. Acceptable gain and efficiency is only evident in the upper end of the input power range.

B. PA Performance

The PA system incorporating predistortion achieves a PAE of 66.4% at 25.90 dBm P_{OUT}. Fig. 11 shows the output spectrum with the predistortion enabled. ACPR1 is $-36/-33$ and ACPR2 is $-47/-47$ dBc. Gain is 10.9 dB. Increasing P_{IN} improves the adjacent channel power ratio (ACPR) suppression slightly, but at the sacrifice of gain and PAE.

The asymmetry experienced in the measured ACPR is partially due to timing misalignment between the RF and envelope paths. The timing between these paths must be critically tuned to ensure accurate synchronization and to minimize the ACPR. In this system, synchronization is achieved approximately by analog delay matching and fine tuned by clock selection in the digital baseband section.

At 25.90 dBm P_{OUT}, the time-domain envelope waveforms were captured (Fig. 12) to display the degradation due to the AD8041 op-amp. The peaks at the envelope modulator output are clipped below the intended 5.1 V. Similarly the nulls do not reduce fully to 0 V. The AD8041 is quoted as having a rail-to-rail output, but this is only the case when driving high impedances. At the substantial output currents necessary for replicating the peaks and nulls, there will be a significant voltage drop.

C. DA Performance

Class E amplifiers have a low gain due to their switching nature. A gain of 10 dB is considered good since most are lower, often less than 6 dB [17]. A switching amplifier with a drain efficiency of 80% and a gain of only 6 dB will result in a PAE of only 67%. Commercial WCDMA PAs, like the ACPM-7311 [18], typically have high gain, and only require a P_{IN} in the order of 0 dBm. This is compatible with most commercial up-converter ICs, which have a maximum P_{OUT} in the order of 0 dBm, e.g., the AK1529. Due to this, a DA is required for practical application.

A linear DA was constructed for this application; it is biased with a 3.6-V supply voltage, as used by the SMPS part of the envelope modulator. To ensure the DA is well matched to 50 Ω for driving the PA appropriately, shunt-series feedback is exploited [19].

A DA output return loss of -20 dB at 15.4 dBm was achieved, with a resulting PAE of 49.1% and an ACPR1 of -35 dBc. A schematic of the DA is shown in Fig. 13. The 2N3904 transistor defines a low-impedance dc bias source since large input RF signals can produce a dc potential at the ATF-54143's gate and upsetting its bias point. The input match of the DA can be manipulated with the trimmer capacitor that, in turn, affects the output match.

D. DA PA Cascade Performance

The transfer response of the cascade DA+PA amplifier under CW excitation is shown in Fig. l4.

The transfer response of Fig. l4 exhibits a significant nonlinearity from -12 to -8 dBm (P_{IN}). This is due to the combination of the PA's class E response and the DA's mildly nonlinear response. The DA's output impedance due to the shunt-series

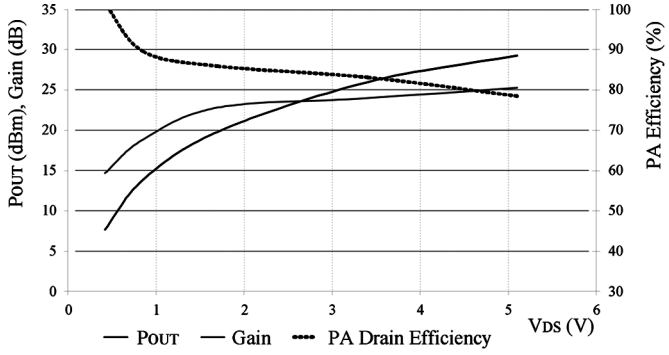

Fig. 15. Cascade amplifier $V_{\rm DS}$ response under CW excitation.

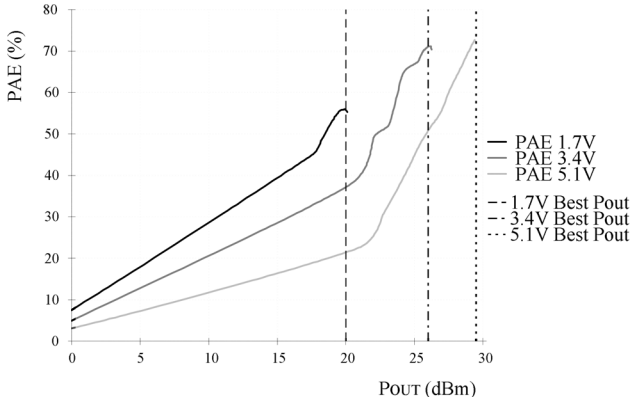

Fig. 16. Cascade amplifier swept PAE response. The output power at which the most efficient operation for different levels of backoff is indicated by vertical hatched traces.

feedback drives the PA into a mode where its drain efficiency approaches 85%.

Fig. 15 shows the relationship between the cascade amplifier $P_{\rm OUT}$, gain, and PA drain efficiency response for a changing $V_{\rm DS}$ with a fixed DA $V_{\rm DS}$. $P_{\rm IN}$ to the cascade amplifier is manipulated so that the expected $P_{\rm OUT}$ is achieved for a given $V_{\rm DS}$. The overall gain is less at lower $V_{\rm DS}$ since a moderate level of $P_{\rm IN}$ is still required to drive the PA into saturation. The PA's efficiency appears to increase at low $V_{\rm DS}$; however, this is due to the carrier signal leaking across the transistor.

E. Predistortion Calculation

Fig. 15 shows that the cascaded amplifier's gain response is nonlinear, suggesting that a fully modulated carrier cannot be used directly since it will not drive the amplifier appropriately at all levels of $V_{\rm DS}$. At the same time, the gain does not directly follow the $P_{\rm OUT}$ response, suggesting that a constant envelope carrier would also not be appropriate. The input signal must, therefore, contain some amplitude modulation to achieve the correct $P_{\rm OUT}$, and hence, maximize the PAE at all values of $V_{\rm DS}$.

Since $V_{\rm OUT}$ (derived from $P_{\rm OUT}$) of a class E amplifier is directly proportional to $V_{\rm DS}$, given the appropriate value of $P_{\rm IN}$, a class E amplifier can be said to have a linear dc power to RF power response. If $P_{\rm IN}$ is too small, the transistor will not switch correctly between the saturation region and nonconduction. Ideally the class E amplifier should have a 50% duty cycle; if $P_{\rm IN}$ is too large, then the duty cycle will be greater than 50%, leading to sub-optimum operation. This will reduce PAE, and the gain since a portion of $P_{\rm IN}$ is now wasted.

Fig. 16 shows the swept $P_{\rm OUT}$ response for the cascade amplifier at 1.7 $V_{\rm DS}$ (6-dB backoff), 3.4, and 5.1 V (3.5-dB peak). Each of the PAE curves peak at their corresponding $P_{\rm OUT}$: 20, 26, and 29.5 dBm. To ensure that the dc power to RF power linearity is maintained, alongside a high PAE, the peak of the PAE curves should intersect their corresponding best $P_{\rm OUT}$ line.

At the intersection of the PAE curves and the best $P_{\rm OUT}$ lines, the gain is reduced from that of its peak. At 5.1 V, the gain is 10 dB down from its peak gain with a corresponding PAE of only 41%.

The optimum $P_{\rm OUT}$ of the amplifier with a $V_{\rm DS}$ of (26 dBm) is specified as the peak PAE $P_{\rm OUT}$. Since the PAE is a factor of the gain, the gain must also be considered when evaluating amplifier performance. Because of the linear dc power to RF power response, the peak PAE $P_{\rm OUT}$'s are in the appropriate place for $V_{\rm DS}$'s of 1.7 and 5.1 V.

The predistortion is chosen so that an appropriate $P_{\rm OUT}$ is achieved for a given $V_{\rm DS}$. An appropriate $P_{\rm IN}$ may also be determined for a particular $V_{\rm DS}$ from Fig. 16. It can be seen, that at 3.4 V, $P_{\rm IN}$ ($P_{\rm OUT}$ minus gain) is 1 dBm. At 1.7 and 5.1 V, it is -3 and 3 dBm, respectively. The $P_{\rm IN}$ to $P_{\rm OUT}$ relationship is nonlinear. This relationship necessitates predistortion if linear amplification and the ACPR mask is to be achieved. By taking a number of points on the $V_{\rm IN}$ (derived from $P_{\rm IN}$) and $V_{\rm DS}$ curve, a polynomial amplitude predistortion equation may be derived. In this demonstrator, the amplifier characteristics were measured in order to determine the predistortion characteristics; in a production environment, this process may be automated at handset commissioning. The coefficients of this polynomial equation may either be implemented in real time at the baseband, or used to calculate a lookup table for offline real-time mapping.

Although the combined polar modulator and class E amplifier exhibits a nonlinear transfer characteristic, it is significantly more linear than that of the class E amplifier in isolation. As a result, the predistortion need only provide 5–6 dB of linearity improvement. This modest linearity improvement demand makes the variations in the transistor's characteristics due to supply voltage, input signal power, temperature, and frequency acceptable.

F. System Performance Under WCDMA Excitation

Fig. 17 shows the output spectrum of the cascade amplifier and envelope modulator with and without predistortion. $P_{\rm IN}$ is 2 dBm and $P_{\rm OUT}$ is 26.05 dBm, yielding 24 dB of gain. $\rm PAE_{overall}$ is 60% and the PA efficiency 82.4%. Without predistortion, the ACPR1 is -32.1 and -31.4 dBc, and ACPR2 is -40.6 and -40.2 dBc. The predistortion improves the ACPR1 to -35.3 and -37.5 dBc, and the ACPR2 to -49.3 and -48.3 dBc. The WCDMA mask is also shown in Fig. 17.

There is a slight asymmetry to the spectrum caused by two phenomena. The first is residual timing misalignment between the envelope and RF paths after tuning resulting in the envelope and RF carrier combining incorrectly. The second, and more dominant, is the asymmetric clipping of the RF carrier by the

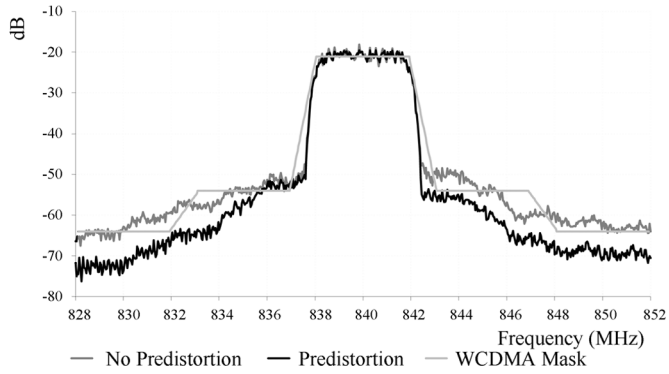

Fig. 17. WCDMA amplifier spectrum with ACPR guides. At peak output power the spectrum with predistortion is shown to be compliant with the standard requirements.

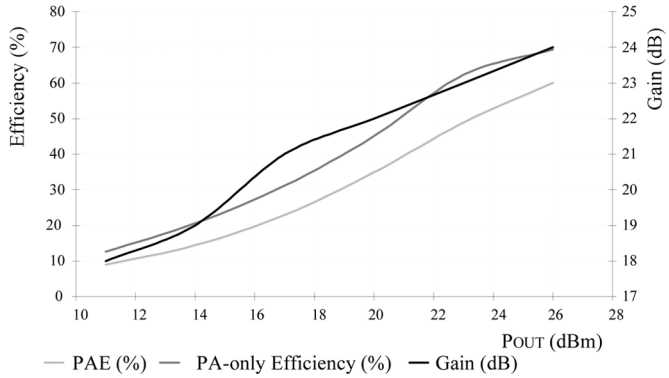

Fig. 18. PA PAE, system efficiency, and gain for the cascade polar modulator amplifier under backoff for WCDMA excitation. At peak output power of +26 dBm, an overall efficiency of 60% is shown.

DA. This will change the duty cycle at which the class E PA switches.

The amplifier is intended for high-efficiency peak performance. Often, under normal conditions for a WCDMA handset, the amplifier operates at a lower P_{OUT}; 10- or 20-dB backoff is common. It is important that the amplifier maintains a high degree of performance under backoff. By reducing the supply voltage and sweeping P_{IN} of a modulated input, the optimum performance can be determined for maximum PAE. The results for amplifier PAE, PA-only efficiency, and gain are shown in Fig. 18.

At backedoff levels of P_{OUT}, the predistortion will fit the amplifier characteristics less accurately, as it is optimized for peak power performance, and also the error of the envelope modulator becomes more prominent. These two errors manifest themselves as a reduction in the ACPR ratio, as shown in Fig. 19 (the standard limits are also shown).

Fig. 19 in combination with Fig. 18 gives an indication of when, under backoff, the switch mode PA should be disabled and a linear PA used instead. The ACPR2 specification is only met over a 5-dB P_{OUT} backoff; below this, a linear PA should be used to maintain the ACPR specification. In Fig. 18 the PAE at 5-dB backoff P_{OUT} is reduced to 40%, equivalent to that of a linear amplifier. There is no justification in operating the polar modulator under backoff when its PAE is equivalent or less than that of a linear amplifier.

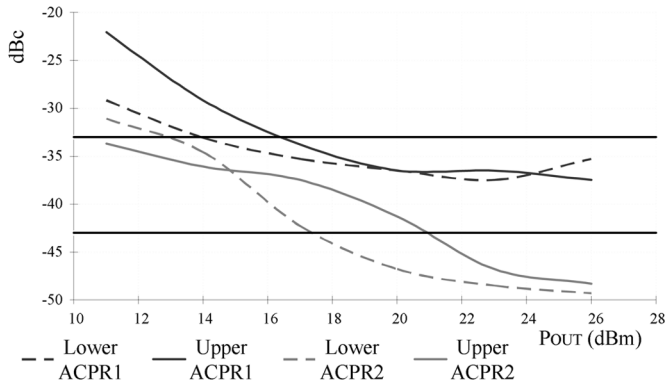

Fig. 19. Cascade polar modulator amplifier ACPR under backoff. The solid horizontal lines represent the standard requirements for ACPR1 and ACPR2. The architecture is standard compliant for the upper 10 dB of the output power range.

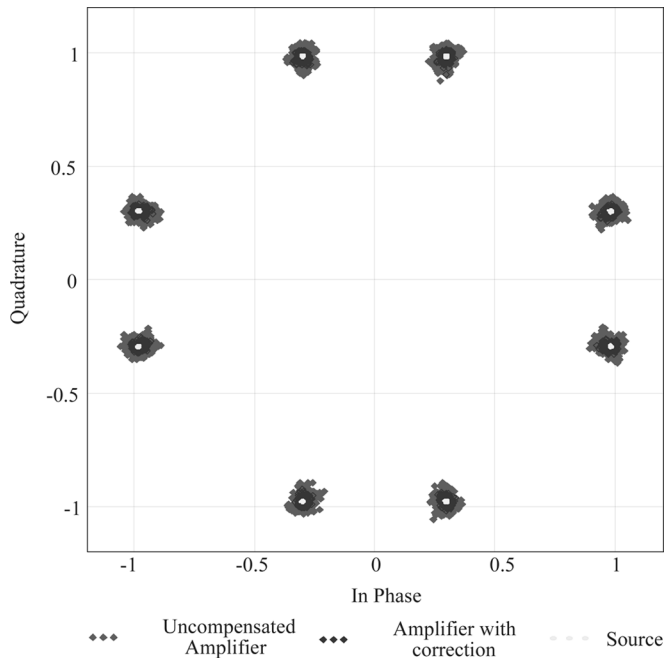

Fig. 20. Constellation diagram of signal generator (source) and cascade amplifier (26-dBm P_{OUT} at 840 MHz). With correction, an amplifier system EVM of 2% is achieved. Measurements taken with support from the National Physical Laboratory, Middlesex, U.K.

The ACPR performance of Fig. 19 may be improved with adaptive pre-distortion to better match the amplifier's characteristics under backoff. This could also improve the PAE since the PA will be driven in a more appropriate mode, and hence, improve the backedoff PAE.

The WCDMA baseband I and Q signals were generated in Agilent ADS [20], a separate envelope signal was derived, and predistortion applied to the RF carrier. Measuring the cascade amplifier and envelope modulator with the predistorted signal derived from Fig. 17, the EVM is 2.0%. Fig. 20 shows the constellation diagram of the un-predistorted signal generator (source) and cascade amplifier with (corrected) and without (uncompensated) predistortion. The EVM without predistortion is 3.9%.

VI. Conclusion

This paper has reported the design and performance of a handset WCDMA transmitter amplifier that is standard compliant, yet far exceeds the peak power PAE available from conventional systems. An efficiency enhancement has resulted from a new technique employed in the envelope modulator; namely, splitting the information content in the frequency domain and employing feedback to ensure that each part is amplified by a system that is most suited to it. A further efficiency enhancement has resulted in a digression from the standard carrier-limiting approach of an EER system so that the amplitude of the carrier tracks the envelope amplitude in a relationship that keeps the class-E amplifier in its most efficient mode while promoting a linear translation of drain voltage to output envelope voltage.

The performance of each subsystem is reported in isolation and the overall system is shown to be standard compliant with a peak power PAE of 60%.

References

[1] S. Im and E. J. Powers, "An application of a digital predistortion linearizer to CDMA HPAs," in *IEEE Global Telecommun. Conf.*, 29 Nov.–3 Dec. 2004, vol. 6, pp. 3907–3910.

[2] L. R. Kahn, "Single-sideband transmission by envelope elimination and restoration," *Proc. IRE*, vol. 40, no. 7, pp. 803–806, Jul. 1952.

[3] J.-F. Bercher and C. Berland, "Envelope/phase delays correction in an EER radio architecture," in *13th IEEE Int. Electron., Circuits, Syst. Conf.*, Dec. 10–13, 2006, pp. 443–446.

[4] N. D. Lopez, Xufeng Jiang, D. Maksimovic, and Z. Popovic, "Class-E power amplifier in a polar EDGE transmitter," in *IEEE MTT-S Int. Microw. Symp. Dig.*, Jun. 11–16, 2006, pp. 785–788.

[5] D. Milosevic, J. von der Tang, and A. van Reormund, "On the feasibility of applications of class E RF power amplifiers in UMTS," in *Proc. IEEE Circuits Syst. Int. Symp.*, May 25–28, 2003, vol. 1, pp. I149–I152.

[6] A. Grebennikov, "Load network design technique for class E RF and microwave amplifiers," *High Freq. Electron.*, pp. 18–32, Jul. 2004.

[7] L. Negra and W. Bachtold, "Lumped-element load-network design for class-E broadband class-E power amplifiers," *IEEE Trans. Microw. Theory Tech.*, vol. 54, no. 6, pp. 2684–2690, Jun. 2006.

[8] N. O. Sokal and A. D. Sokal, "Class E-A new class of high efficiency tuned single-ended switching power amplifiers," *IEEE J. Solid-State Circuits*, vol. SC-10, no. 3, pp. 168–176, Jun. 1975.

[9] "ATF-501 datasheet," Avago Technol., San Jose, CA, 2004. [Online]. Available: www.avagotech.com

[10] B. Sahu and G. A. Rincón-Mora, "A high-efficiency, linear RF power amplifier with a power-tracking, dynamically adaptive buck-boost supply," *IEEE Trans. Microw. Theory Tech.*, vol. 52, no. 1, pp. 112–120, Jan. 2004.

[11] F. Wang, A. Ojo, D. Kimball, P. Asbeck, and L. Larson, "Envelope tracking power amplifier with pre-distortion for WLAN 802.11g," in *IEEE MTT-S Int. Microw. Symp. Dig.*, 2004, pp. 1543–1546.

[12] N. Wang, X. Peng, V. Yousefzadeh, D. Maksimovic, S. Pajic, and Z. Popovic, "Linearity of X-band class-E power amplifiers in EER operation," *IEEE Trans. Microw. Theory Tech.*, vol. 53, no. 3, pp. 1096–1102, Mar. 2005.

[13] "OPA357 datasheet," Texas Instruments Incorporated, Dallas, TX, 2002. [Online]. Available: www.ti.com

[14] "AD8605 datasheet," Analog Devices, Norwood, MA, 2001. [Online]. Available: www.analog.com

[15] "AD8041 datasheet," Analog Devices, Norwood, MA, 1993. [Online]. Available: www.analog.com

[16] "MAX1820 datasheet," Maxim IC, Portland, OR, 2001. [Online]. Available: www.maxim-ic.com

[17] E. W. Bryerton, M. D. Weiss, and Z. Popovic, "Efficiency of chip-level versus external power combining," *IEEE Trans. Microw. Theory Tech.*, vol. 47, no. 8, pp. 1482–1485, Aug. 1999.

[18] "BA1232 datasheet," Mitsubishi Elect. Semiconduct., San Jose, CA, 2007. [Online]. Available: www.mitsubishichips.com

[19] R. G. Meyer, R. Eschenbach, and R. Chin, "A wide-band ultralinear amplifier from 3 to 300 MHz," *IEEE J. Solid-State Circuits*, vol. SC-9, no. 4, pp. 167–175, Aug. 1974.

[20] Advanced Design System (ADS) Agilent Technol., Santa Clara, CA, 2009. [Online]. Available: www.agilent.com

Paul A. Warr received the B.Eng. degree in electronics and communications from The University of Bath, Bath, U.K., in 1994, and the M.Sc. degree in communications systems and signal processing and Ph.D. degree from The University of Bristol, Bristol, U.K., in 1996 and 2001, repectively. His doctoral dissertation concerned octave-band linear receiver amplifiers.

He is currently a Senior Lecturer of electronics with the University of Bristol. His research concerns the front-end aspects of software (reconfigurable) radio and diversity-exploiting communication systems, responsive linear amplifiers, flexible filters, and linear frequency translation. His research has been supported by the U.K. Department of Trade and Industry (DTI)/Engineering and Physical Sciences Research Council (EPSRC) alongside European Commission programs and industrial collaborators.

Kevin A. Morris received the B.Eng. and Ph.D. degrees in electronics and communications engineering from the University of Bristol, Bristol, U.K., in 1995 and 1999, respectively.

In 1998, he became a Research Associate with the Centre for Communications Research (CCR), University of Bristol, during which time he was involved in a number of projects including the Engineering and Physical Sciences Research Council (EPSRC) PACT LINK Program and the Information and Communication Technologies (IST) project SUNBEAM. In 2001, he became a Lecturer in RF engineering with the University of Bristol, and in August 2007, became a Senior Lecturer. He is currently involved with a number of research programs within the U.K. including the Mobile VCE Core 5 Research Program. He has authored or coauthored 14 academic papers. He co-holds three patents. His research interests are in the area of RF hardware design with a specific interest in the design of efficient linear broadband PAs for use within future communications systems.

Gavin T. Watkins received the M.Eng. and Ph.D. degrees in electrical and electronic engineering from the University of Bristol, Bristol, U.K., in 2000 and 2003, respectively. His doctoral dissertation concerned the investigation of broadband tunable feedforward amplifiers for software defined radio front-ends.

From 2003 to 2004, he was an Engineering Consultant for Detica Information Intelligence, during which time he was involved with various RF and analog projects. From 2004 to 2008, he was a Research Associate with the University of Bristol, where he was involved in the investigation of high-efficiency EER class E based PAs for WCDMA. In 2008, he joined Toshiba Research Europe Limited, Bristol, U.K., as a Senior Research Engineer, where he currently investigates CMOS millimeter-wave transceiver circuitry. His current research interests include switching amplifiers, low-power broadband CMOS circuits, and efficient signal envelope modulators.

Tony R. Horseman received the B.Eng. and Ph.D. degrees from the University of Bristol, Bristol, U.K., in 1994 and 1999, respectively.

He is currently a Research Fellow with the Centre for Communications Research (CCR), University of Bristol. His areas of interest include the prototyping of advanced or novel systems, linearized RF, multiple input multiple output (MIMO), and wireless local area networks (WLANs).

Kaoru Takasuka was born in Hiroshima, Japan, in 1947. He received the B.S. and M.S. degrees in instrumentation engineering from the Kyushu Institute of Technology, Kitakyushu, Japan, in 1970 and 1972, respectively.

In 1972, he joined Asahi Kasei. Since 1983, he has been engaged in the design of custom CMOS large-scale integrated circuits (LSICs). He is currently the CTO of the Asahi Kasei EMD Corporation, Tokyo, Japan.

Mr. Takasuka was a corecipient of the 1986 Technical Excellence Award presented by the Society of Instrument and Control Engineers of Japan and the Institute of Electrical Engineers of Japan 2001 Millennium Best Paper Award.

Yukihiro Ueda was born in Fukuoka, Japan, in 1957. He received the B.S. and M.S. degrees in control engineering from the Kyusyu Institute of technology, Kitakyushu, Japan, in 1980 and 1982, respectively.

In 1982, he joined Asahi Kasei. Since 1987, he has been engaged in the design of custom CMOS large-scale integrated circuits (LSICs). He is currently the Special Function Analog Unit Manager with the Asahi-Kasei EMD Corporation, Kanagawa, Japan. His current research interests are low-noise mixed-signal LSICs.

Yasushi Kobayashi was born in Tokyo, Japan, in 1958. He received the B.S. and M.S. degrees in material engineering from Keio University, Tokyo, Japan, in 1982 and 1984, respectively.

In 1984, he joined Asahi Kasei. He has been engaged in the design of custom CMOS large-scale integrated circuits (LSICs). He is currently the Multi-Media Group Section Manager of the Asahi-Kasei EMD Corporation, Kanagawa, Japan. His current research interests are low-noise mixed-signal LSICs.

Shinji Miya was born in Kanagawa, Japan, in 1962. He received the B.S. degree in basic science from the University of Tokyo, Tokyo, Japan, in 1987, and the M.S. degree in electronic engineering from King's College, London, U.K., in 1997.

In 1987, he joined Asahi Kasei. Since 1997, he has been engaged in custom RF integrated circuit (RFIC) design for mobile phones. He is currently a Staff Engineer with the Asahi-Kasei EMD Corporation, Kanagawa, Japan. His current research interests are highly integrated RF large-scale integrated circuits (LSICs).